FUNCTIONALISED a-C COATINGS TO REDUCE SEY AND CONTROL SURFACE RESISTANCE FOR THE HL-LHC INJECTION KICKER BEAM-PIPE CERAMIC SUPPORTS

P. Costa Pinto, G. Favia, C. Kouzios, M. Himmerlich, L. Mourier, W. Vollenberg
European Organization for Nuclear Research, Geneva, Switzerland
N. Bundaleski, I. Ferreira, D. Galhano, Universidade Nova de Lisboa, Lisbon, Portugal
P. Guerreiro, Centro de Física e Investigação Tecnológica, Caparica, Portugal
A. Costa, Centro de Ciências e Tecnologias Nucleares, Bobadela, Portugal

Abstract

Functionalized amorphous carbon (a-C) coatings are being developed to reduce the secondary electron emission yield (SEY) and to control the surface resistance of ceramic supports for the new generation of HL-LHC injection kicker magnets. Pressure spikes observed during high-voltage pulsing of the new injection kicker magnets are attributed to flashovers caused by high electron emission and insufficient draining of surface charge on the alumina supports of the beam-pipe. To address this issue, the alumina supports for the next generation of injection kicker magnets are coated with an a-C film, providing suitable surface resistivity to prevent charge accumulation whilst preserving the insulating function of the supports, together with a low SEY.

This contribution reports on the R&D programme aimed at tuning the resistivity of the a-C films through hydrogen doping while maintaining acceptable SEY performance. Results from the production of a series of 25 coated supports are presented, along with complementary studies carried out to optimise the coating pro-cess for future large-scale production. The potential of these resistive a-C films as alternatives to Ti and TiN coatings for insulating components is also discussed.

MANUSCRIPTS

The first units of HL-LHC MKI Cool injection kicker magnets, which have already been installed during the third operational run of the LHC, have demonstrated effective mitigation of beam-induced heat loads and improved vacuum performance [1]. However, pressure spikes during high-voltage pulsing have raised concerns about electron emission from alumina supports due to their high SEY. To address this issue, alumina supports are coated with amorphous carbon (a-C), which must simultaneously provide an SEY significantly lower than alumina (SEY ≈ 4–8) [2], and a surface resistance in the range 0.1–10 MΩ. Very thin a-C films (~5 nm) already exhibit a surface resistance of around 1 MΩ. However, two limitations arise: (i) the minimum thickness required to effectively screen substrate emission is ~10 nm [3], and (ii) at low thickness, surface resistance is highly sensitive to rough-ness and nucleation effects. To decouple thickness and resistance constraints, hydrogen doping is introduced, increasing resistivity and enabling the target surface resistance (~1 MΩ) at thicknesses of ~100 nm. The drawback is that the SEY increases with hydrogen content [4]. This work investigates the resistivity and SEY dependence on hydrogen concentration and thickness, the control via discharge power and the thermal stability under bakeout conditions.

FILM DEPOSITION AND CHARACTERIZATION

Films are deposited by DC magnetron sputtering using graphite targets. The system is baked at 120 °C for 8 hours prior to deposition, reaching ~1×10^{-7} mbar base pressure after cooling. Target–substrate distance is 200 mm and discharge pressure is 8×10^{-3} mbar. Reference films are deposited in pure Ar (60 grade), while doped films use Ar/D_2 mixtures (98.7%/1.3%). Deuterium distinguishes intentional doping from residual hydrogen contamination [4]. Unless stated otherwise, discharge power is 100 W.

Thickness is measured by profilometry, resistivity by four-point probe. The composition of the film is analysed using ion beam analysis combining Rutherford Back Scattering, Elastic Recoil Detection Analysis, and Nuclear Reaction Analysis, Taug gap obtained via optical absorption spectroscopy, and SEY is measured in a dedicated setup (instrumentation and methodologies are described in [4]).

RESISTIVITY AND H DOPING

Figure 1 shows the dependence of surface resistance on thickness for reference and doped films. Reference films reach 1 MΩ at ~5 nm, while doped films require ~70 nm. A sharp decrease in resistance occurs within the first 15–20 nm, attributed to nucleation and surface roughness effects, strongly affecting reproducibility. Figure 2 shows resistivity versus discharge power. Lower discharge power increases hydrogen incorporation, promoting sp^3 bonding and increasing resistivity [5, 6]. Alumina substrates yield 2–5 times higher resistivity than glass due to surface roughness effects.

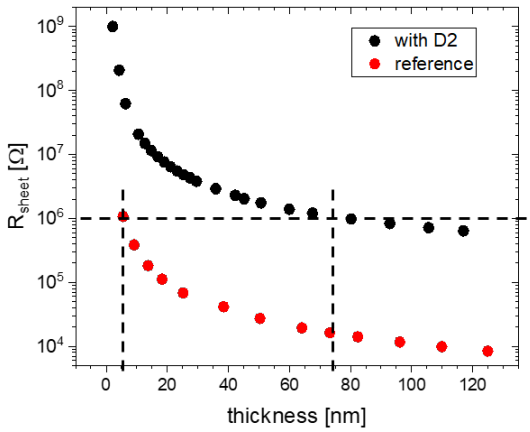

Figure 1: Surface resistance as a function of the thickness for films deposited in pure Ar (reference) and Ar/D2. The samples were deposited on glass substrates at a discharge power of 100 W.

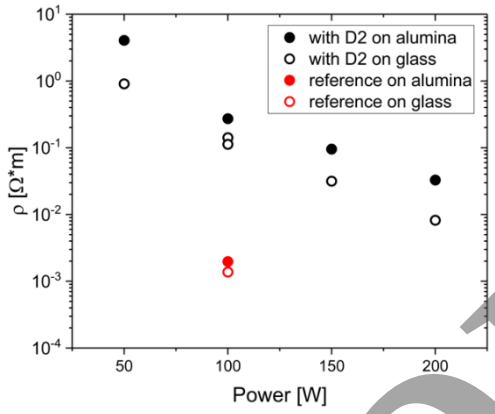

Figure 2: Dependence of the resistivity on the discharge power, for film thicknesses of ~135 nm. Unfilled circles correspond to glass substrates, filled circles to alumina substrates.

A logarithmic dependence between SEY and resistivity is observed (Fig. 3), enabling tuning of electrical properties while maintaining low electron emission.

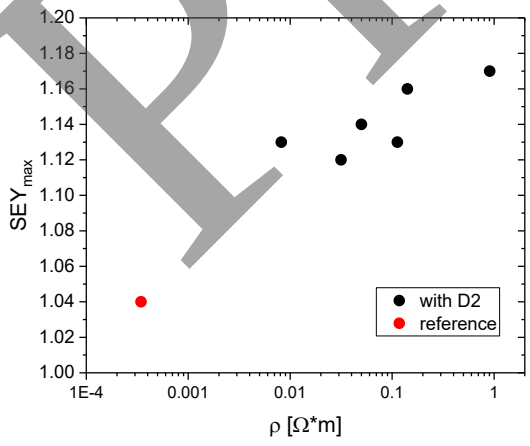

Figure 3: Relation between the SEY and the resistivity.

Figure 4 shows the elemental composition of the films. Hydrogen and deuterium content decrease with increasing discharge power, confirming plasma-controlled doping. No H/D loss is observed after annealing at 260 °C for 125 h.

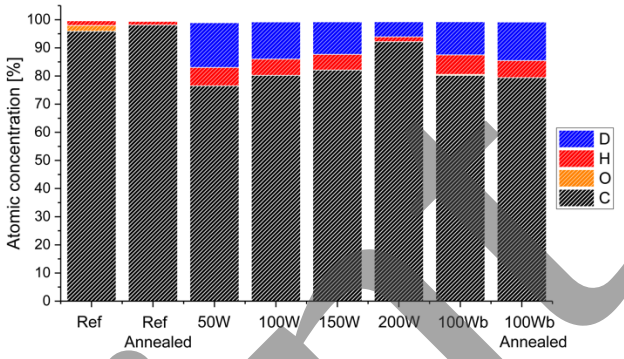

Figure 4: Film composition analysed by ion beam techniques. Ar was also present in all samples, at atomic concentrations below 1%.

THERMAL STABILITY

MKI Cool magnets are baked at 250 °C. Thermal stability was evaluated by cycling films up to 260 °C, holding for 125 h, and cooling to room temperature. A second identical cycle was performed to verify the stability of the resistivity.

Figure 5 shows the resistivity evolution as a function of the baking temperature. During the first heating cycle, resistivity decreases due to annealing and negative temperature coefficient effects typical for graphite-like materials. Stabilisation occurs within ~30 h. After cooling, resistivity stabilises at ~35% of its initial value. The second cycle follows the same trajectory as the first cooldown. These results show that a stable structure is achieved up to 260 °C. Coatings must therefore be de-signed with an initial resistivity ~2.5× higher than the operational specification.

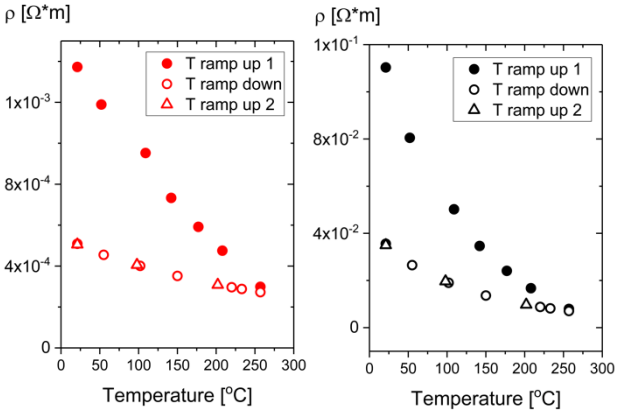

Figure 5: Evolution of the resistivity during thermal cycling for a reference (red) and Ar-D2 coating produced at 100 W.

Figure 6 correlates resistivity with the Tauc gap, reflecting the balance between sp^2/sp^3 bonding in amorphous carbon [6]. Higher hydrogen content increases the sp^3 fraction

and both gap and resistivity [7]. After annealing, the doped sample shows only a slight reduction in Tauc gap despite a strong resistivity de-crease. Since no H/D loss is detected, this is attributed to increased connectivity of sp^2 clusters rather than phase transformation.

The reference sample shows a strong Tauc gap reduction (from ~2.5 eV to ~0.25 eV), consistent with increased sp^2 ordering.

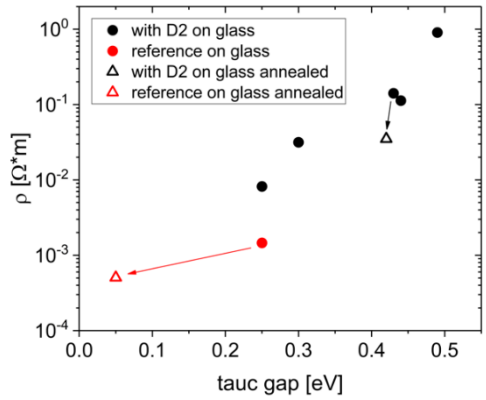

Figure 6: Figure 6: Relationship between the resistivity and the "Tauc" gap. Empty triangles represent values obtained after annealing samples produced at 100 W.

Overall, thermal cycling up to 260 °C reduces resistivity to approximately 35% of its initial value without inducing structural degradation or adhesion concerns.

PRODUCTION OF MKI COOL SUPPORTS

A total of 25 alumina supports were coated in two runs per support to coat both faces. Supports were processed in batches of two (Fig. 7), resulting in 25 full coating runs. Deposition used Ar/H_2 (99.5%/0.5%) at 100 W, targeting ~100 nm thickness.

Figure 7: Alumina supports before (a) and after coating (b).

Quality control included four-point probe measurements at four positions per face and SEY measurements on witness samples. A total of 200 resistivity measurements were recorded.

Figure 8 shows the resistivity distribution across all measured positions, corrected for bakeout effects. All values meet specifications. The inset shows the maxi-mum SEY obtained per coating run.

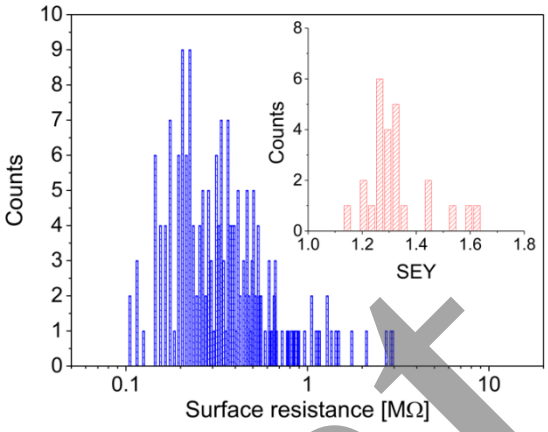

Figure 8: Histogram showing the distribution of the resistivity measured on the supports (corrected for the expected effect of the bakeout). The inset shows the SEY.

CONCLUSIONS

Hydrogen-doped amorphous carbon coatings enable controlled tuning of resistivity while maintaining the SEY significantly lower than for bare alumina, making them suitable for the LHC MKI Cool injection kicker magnet supports. Doping increases resistivity, enabling thicker coatings and reducing sensitivity to roughness, im-proving reproducibility. Initial thermal cycling stabilises film structure and reduces resistivity to ~35% of its initial value.

A total of 25 supports were successfully coated, with all resistivity values within specification and obtaining an average SEY ~1.3. Two coating runs showed higher SEY (~1.6), attributed to hydrogen partial pressure variations during the final deposition stage. These results demonstrate the ability for stable production and highlight the importance of precise hydrogen control for reproducible SEY performance.

Resistive a-C films represent a promising alternative to Ti and TiN coatings for mitigation of multipacting in accelerator vacuum and RF components, due to their lower SEY and the possibility of using thicker coatings (~100 nm instead of ~5 nm for Ti), thereby reducing the impact of surface roughness variability on the surface resistance.

REFERENCES

[1] G. Favia *et al*., "Operational experience and design improvement studies of the LHC MKI Cool", in *Proc. IPAC'25,* Taipei, Taiwan, Jun. 2025, pp. 466-469. doi:10.18429/JACoW-IPAC2025-MOPM064

[2] Suharyanto *et al.*, "Secondary electron emission and surface charging evaluation of alumina ceramics and sapphire", *IEEE Trans. Dielectr. Electr. Insul.,* vol. 13, no. 1, Feb. 2006. doi:10.1109/TDEI.2006.1593403

[3] M. Angeluci *et al.*, "Minimum thickness of carbon coating for multipacting suppression", *Phys. Rev. Res.,* vol. 2, no. 3, p. 032030(R), Aug. 2020. doi:10.1103/PhysRevResearch.2.032030

[4] C. F. Adame *et al.*, “Amorphous carbon thin films: Mechanisms of hydrogen incorporation during magnetron sputtering and consequences for secondary electron emission”, *J. Vac. Sci. Technol. A*, vol. 41, no. 4, p. 043412, 2023. doi:10.1116/6.0002759

[5] P. Costa Pinto *et al.*, “Mitigating the detrimental effect of hydrogen impurities on the secondary electron yield of amorphous carbon thin films: A study on power density and discharge modes”, *Surf. Coat. Technol.,* vol. 517, 132841 Dec. 2025. doi:10.1016/j.surfcoat.2025.132841

[6] J. Roberston, “Diamond-Like amorphous carbon”, *Mater. Sci. Eng. R. Rep.*, vol. 37, no. 4-6, pp. 129-281, May 2002. doi:10.1016/S0927-796X(02)00005-0

[7] N. Bundaleski *et al*., “The role of hydrogen incorporation into amorphous carbon films in the change of the secondary electron yield”, *Int. J. Mol. Sci.*, 2023, vol. 24, no. 16, p. 12999, Aug. 2023. doi:10.3390/ijms241612999